Optical power monitor using a thin-film pyroelectric bimorph

S. B. Peralta, K. Ghandi, and A. Mandelis

Photoacoustic and Photothermal Sciences Laboratory, Department of Mechanical Engineering, University of Toronto and Ontario Laser and Lightwave Research Center, Toronto, Ontario M5S 1A4, Canada

(Received 4 October 1989; accepted for publication 13 November 1989)

A novel pyroelectric detector, based on a bilayer laminate of pyroelectric thin films, is described. A theoretical analysis shows that this detector element, which is called a pyroelectric bimorph, has the potential of having a higher sensitivity than an equivalent single-element detector. Verification of this result was found by characterizing three bimorph detectors based on polyvinylidene fluoride (PVDF). The specific detectivity for one particular bimorph was measured to be 6.6×10^{8} cm $Hz^{1/2}/W$, at a modulation frequency of 1 Hz, approximately twice the reported value for a single-element pyroelectric polymer film. We discuss operating characteristics for the three pyroelectric bimorph elements and evaluate their use in optical power monitoring.

INTRODUCTION

Conventionally, the materials most used in pyroelectric detectors have taken the form of single crystals such as triglycine-sulphate (TGS), lithium tantalate (LT), strontium barium niobate (SBN), and ceramics such as lead zirconate titanate (PZT). In recent years, however, polymer films such as polyvinyl fluoride (PVF), polyvinylidene fluoride (PVDF) and polyvinylidene fluoride trifluoroethane (PVDF/TrFe) have come into increasing use as detector elements in pyroelectric devices.[1,2] Among the advantages of such polymer films over single crystal and ceramic materials are that they are flexible and robust, and can be produced in large areas which require little processing, and are therefore inexpensive. These materials may also be compared as to suitability as a detector element through a figure of merit[3] $M=(p/\epsilon C)$, where p is the pyroelectric coefficient, ϵ the dielectric constant and C the specific heat of the material. Although the values for p for polymers are an order of magnitude smaller than those of single crystal and ceramic materials, the corresponding values for ϵ are smaller. Furthermore, the thickness of the polymer films may be easily adjusted to minimize the heat capacity. Thus, the differences in the figures of merit for all materials are not very large; for example,[1] $M_{\mathrm{TGS}}=2.8\times10^{-10}$ C J/cm, while $M_{\mathrm{PVDF}}=0.87\times10^{-10}$ C J/cm. Of the polymer films enumerated above, PVDF has the highest figure of merit, as well as the highest pyroelectric coefficient, and thus it has been the subject of considerable attention.

In this article we describe a pyroelectric detector element based on a novel configuration of such pyroelectric polymer films; in the present experiments we specifically focus on PVDF as the pyroelectric material. The detector element is based on a bilayer laminate of the polymer film, and can be shown to have a higher theoretical responsivity than for an equivalent single-element detector of the same pyroelectric materials. Because the bilayer laminate configuration is similar to that of the more familiar piezoelectric bimorph,[4] we call the detector element a pyroelectric bimorph. We discuss the operating characteristics of three different pyroelectric bimorphs, and evaluate the use of these devices for monitoring optical power.

I. DESCRIPTION OF THE DEVICE

At thermal equilibrium, the surface charges due to the internal polarization of a pyroelectric material are either neutralized by space charges or discharged by electrical conduction. However, if radiation is incident on the material, the temperature of the pyroelectric materials changes, and so does its internal polarization. The resulting surface charges may then be detected before they are again neutralized.

It is convenient to discuss the operation of the pyroelectric bimorph in terms of the more familiar piezoelectric bimorph.[4] First, consider a single-element piezoelectric polymer film. An applied voltage across its thickness z changes its dimension in length, width, and thickness, to a degree proportional to the original dimensions and the applied voltage. Since such films are usually only a few microns thick, the change along the x-y direction is orders of magnitude greater than along z. This bending effect may be enhanced by a special film configuration, called the bimorph. Bimorphs consist of two film layers bonded together and connected such that an applied voltage causes one film to extend in length and the other to contract, similar to a bimetallic strip. The motional displacement of a bimorph in response to a given applied voltage is several times greater than for a single-layer film. Conversely, mechanical bending of a bimorph causes it to develop a greatly increased output voltage.

The bimorph configuration has been used for some time as a flexural element in ceramic and crystal resonator designs.[4] However, it is only recently that polymer films have been used in this regard,[5] and specifically PVDF, which has been shown to have one of the highest piezoelectric coefficients for all such films.[6–8] These elements have been found useful in sensors and actuators[9,10]; a number of useful reviews can be found in the literature.[1]

 0034-6748/90/031038-06$02.00

In fact, it was the report of the large piezoelectric coefficient in PVDF that prompted investigation of the pyroelectric properties of this particular film.[11] As has been observed above, in addition to having a high piezoelectric coefficient, PVDF also exhibits one of the highest pyroelectric coefficients among polymer films. Furthermore, it has been shown that under illumination, the pyroelectric signal level in PVDF films is several orders of magnitude higher than the piezoelectric signal.[12] Similar observations ruling out piezoelectric contributions to laser-irradiated PVDF films, with the detector operating in the pyroelectric mode, have been reported previously.[13,14] If in the piezoelectric mode bimorphs exhibit a greater electromotional effect than single-element piezoelectric transducers, it turns out, as will be shown below, that the use of such bimorphs in the pyroelectric mode leads to a current output greater than that for a single-element pyroelectric film. Consequently, the responsitivity of such a device is greater than that of conventional pyroelectric detectors. This is the basis for our device.

Figure 1 shows a schematic diagram of the pyroelectric bimorph element. In this study, three types of bimorphs were tested, based on three commercially-available piezoelectric bimorph electromechanical actuators (Pennwalt Kynar BDT1-009A, BDT1-028K, BDT1-028A), which we label B1, B2, and B3, respectively, for convenience. All bimorphs consisted of two PVDF films of dimensions 40×15 mm^2, metallized on either surface and bonded together to form a composite film varying from 9 to 28 μm in thickness. The polarizations of the two layers were arranged antiparallel to each other, but the intersurface electrode layers were connected in parallel, as shown in Fig. 1. Table I summarizes the particular characteristics of each bimorph.

The bimorph is laminated and then coated on the illuminated surface with a thin absorbing layer. This is necessary because light absorption in thin polymer films is small and nonuniform, especially in the infrared region. Therefore, the incident light must be absorbed at the front surface.[1] In the experiments reported we have used matt black enamel paint, sprayed on as a thin coating; we have also tested other black absorbers, with similar results. The bimorph is then backed by a glass slide, and its edges constrained so as to minimize flexural movement and thus any piezoelectric signal from the material. Operationally, the fixing of the bimorph transducer was arranged so that any signal due to the piezoelectric effect was minimized on the screen of the monitoring oscilloscope.

Other dual-element pyroelectric devices have been described previously,[15] but the second element in these devices has been used simply to compensate for any spurious output

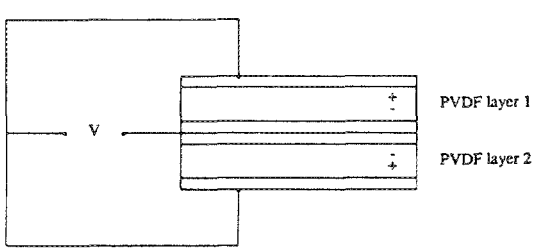

FIG. 1. Schematic diagram of pyroelectric bimorph element.

TABLE I. Physical characteristics of the pyroelectric bimorph detectors.

Bimorph	Type	Dimensions (mm^2)	Thickness (μm)	Metallization
$B1$	BDT1-009A	40×15	9	Ni-Ag
$B2$	BDT1-028K	40×15	28	Ag ink
$B3$	BDT1-028A	40×15	28	Ni-Ag

voltages in the primary element due to environmental effects such as rapid changes in the ambient temperature. Furthermore, these devices differ from ours in that the compensating pyroelectric element is reverse-poled but connected in series with the primary detector element. Such a configuration tends to degrade the detector responsitivity and detectivity.[15] Furthermore, the secondary element in these devices is screened so that it is neither optically nor thermally active; only the primary element serves as the active detector. In our device, the reverse-poled secondary element is connected parallel to the primary element; furthermore, the two are face-connected so that heat conduction through the first layer renders the second layer active as well.

II. THEORY OF DETECTION

A. Pyroelectric detection

Operated in the current mode, pyroelectric devices—unlike other thermal detectors for optical radiation such as thermopiles, bolometers, and the Golay cell—respond to the rate of change of temperature, rather than the actual temperature rise.[16] Thus pyroelectric devices do not have a response for continuous radiation, but rather are operated in an ac mode at a frequency high enough to prevent stray charge from neutralizing the effect before it is measured. This sets a limit at the low end of frequency operation, which depends on the particular detector involved.[2] For continuous or slowly-varying radiation, therefore, intensity-modulation through a mechanical chopper, electro-optical or acousto-optic modulator should be employed.

Consider an ac-modulated laser beam incident on a single-element pyroelectric detector. The incident laser power can be written

$$P = P_0 + P_\omega e^{j\omega t}. \tag{1}$$

If the temperature of the detector increases from T_0 to $T_0 + T_\omega$, it will lose heat to its surroundings at the rate GT_ω, where G is the radiative conductance from the detector. When heat loss is from a single surface of the detector, then $G = 4\eta A\sigma T_\omega^3$; if both sides radiate with the same emissivity, then $G = 8\eta A\sigma T_\omega^3$. Here η is the emissivity of the surface and σ is the Stefan-Boltzmann constant.

Heat balance yields the equation

$$\eta P = H\frac{dT}{dt} + G(T - T_0). \tag{2}$$

$H = C_v Ad$ is the thermal capacity of the detector, C_v is the volume specific heat and d the detector thickness. Thus, the ac temperature component T_ω will be directly proportional to the incident power, given by

$$T_\omega = KP_\omega, \tag{3}$$

where

$$K = \eta(G^2 + \omega^2 H^2)^{-1/2}. \tag{4}$$

Synchronous detection, through a narrowband amplifier—a lock-in amplifier—tuned to the modulation frequency, gives the pyroelectric voltage[17]

$$V(x,t) = (pd/\epsilon)\langle T_\omega(x,t)\rangle. \tag{5}$$

Equation (5) yields a direct measurement of the power of the excitation beam. Here $\langle T_\omega(x,t)\rangle$ is the spatially averaged temperature field in the detector, p is the pyroelectric coefficient, d is the thickness and ϵ the dielectric constant of the detector. For PVDF films, $p = 3\times10^{-5}$ C/m^{2}K and $\epsilon = 12$. The above equations form the basis for the use of pyroelectric detectors as optical power meters. As will be shown below, the same general analysis used for a single-element pyroelectric detector is applicable for a pyroelectric bimorph, with a few important modifications.

B. Equivalent circuit analysis

The equivalent circuit for a pyroelectric bimorph in parallel configuration as in Fig. 1 is shown in Fig. 2(a), where we have explicitly separated the contributions of the two pyroelectric film layers. Each layer is represented as a capacitance C_i in parallel with a resistance R_i, where $i = 1,2$ for the two layers of the bimorph. The alternating charge on the electrodes created by the alternating temperature component due to the modulated laser heating produces an alternating charge $pA\langle T_\omega\rangle_i$ in each layer, equivalent to a current generator $I_i = \omega pA\langle T_\omega\rangle_i$ in parallel to each capacitance. R_A and C_A are the resistance and capacitance of the preamplifier stage, while the amplifier symbol A denotes the circuit of the current amplifier stage used in this work.

The bimorph circuit of Fig. 2(a) reduces to the circuit shown in Fig. 2(b), where the bimorph capacitance C_B is the combined capacitance of the two layers

$$C_B = C_1 + C_2 = 2C_{\rm PVDF}, \tag{6}$$

where $C_{\rm PVDF}$ is the capacitance of a single PVDF film equivalent to one bimorph layer. In the second equality, we have assumed that both bimorph layers are equivalent, that is, that their dimensions and thermal characteristics are the same. The internal bimorph resistance R_B is the combined resistance of the two layers

$$R_B^{-1} = R_1^{-1} + R_2^{-1} = 2R_{\rm PVDF}^{-1}, \tag{7}$$

where $R_{\rm PVDF}$ is the internal resistance of a single equivalent PVDF film, as above. We have neglected in Fig. 2(a) the small contact resistance between the two bimorph layers.

The two current generators of Fig. 2(a) combine to yield a total bimorph current

$$I_B = \omega pA(\langle T_\omega\rangle_1 + \langle T_\omega\rangle_2). \tag{8}$$

The bimorph voltage is then

$$V_\omega = I_B R(1 + \omega^2\tau_E^2)^{-1/2}, \tag{9}$$

where the parameters τ_E, C, and R are given by

$$\tau_E = RC, \tag{10}$$

$$C = C_B + C_A, \tag{11}$$

$$R^{-1} = R_B^{-1} + R_A^{-1}. \tag{12}$$

Now, Fig. 2(b) is simply the equivalent circuit for a single-element pyroelectric detector, except that the values for the circuit elements I_B, C_B, and R_B are as given above, combinations of the single-element values. Thus from the above discussion we can see that a pyroelectric bimorph functions as an ordinary pyroelectric detector, except that the current output of the bimorph detector will always be greater than that of the single-element detector by an amount $\omega pA\langle T_\omega\rangle_2$. Therefore, the responsitivity $\rho = V_\omega/P_\omega$ of a pyroelectric bimorph, will in general be superior to that of a single-element detector.

For bimorphs consisting of thin individual layers, the temperature in the second layer may be treated as equal to the temperature in the first layer, so that the bimorph current approaches a value that is twice the single-element current, following Eq. (8). However, this is not always true for bimorphs in which the individual pyroelectric layers are of arbitrary thickness. In practice, the modulation of incident radiation on a material surface $x = 0$ creates a modulated temperature source at a depth x below the surface given by

$$T(x,t) = T\exp(-x/\mu)\cos(\omega t - x/\mu), \tag{13}$$

where T is the amplitude of the ac temperature at the surface and μ is the thermal diffusion length in the material given by $\mu = (2\alpha/\omega)^{1/2}$ where α is the material thermal diffusivity.

From the above equation, at a depth $x = \mu$, the amplitude of the temperature change will be reduced to $1/e$ of its value at the surface. Thus the advantage of a higher current output in bimorph detectors is reduced as one goes to thicker and thicker individual layers. Since the thermal diffusivity of PVDF film is given by $\alpha = 6\times10^{-8}$ m^2/s, at 100 Hz, $\mu = 13\,\mu$m, while at 10 Hz, $\mu = 44\,\mu$m. From Table I, we see that the total thicknesses of the bimorphs $B1$, $B2$, and $B3$ used here are 9, 28, and 28 μm, respectively, still much thinner than the diffusion lengths at 10 and 100 Hz. However, at higher frequencies the current source advantage of the bimorphs over a single-element detector will be negligible.

To further characterize the device, we made several measurements of the pertinent electrical parameters of the

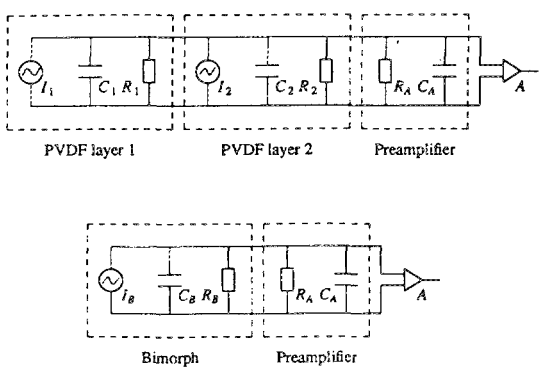

FIG. 2. (a) Equivalent circuit for pyroelectric bimorph. (b) Reduction of circuit 2(a), showing equivalence of pyroelectric bimorph to single-element pyroelectric detector, with correspondingly new values for the current source, internal resistance, and capacitance.

equivalent circuit in Fig. 2(b). To measure the input resistance of the amplifier stage, a dc voltage was first applied to the input of the amplifier, and then through a resistor of value $R_x = 1$ GΩ. The input resistance of the amplifier R_A may then be obtained from

$$R_A = [U_R/(U - U_R)]R_x, \tag{14}$$

where U_R is the dc voltage across the output of the amplifier without resistor R_x, and U_R the dc voltage across the output of the preamplifier with resistance R_x in series with R_A. This yielded the value $R_A = 400 \pm 80$ GΩ. In order to determine C_A, an ac voltage was applied directly to the preamplifier and then through a resistor of value $R_x = 200$ MΩ. The input capacitance of the preamplifier C_A may then be obtained from the equation

$$C_A = (\omega R)^{-1}[(U/U_R)^2 - 1]^{1/2}. \tag{15}$$

This yielded the value $C_A = 16 \pm 3$ pF. While the resistance of the cable connecting the bimorph stage to the amplifier stage was negligible in comparison to the measured R_A of the amplifier, its capacitance was found to be 140 ± 2 pF. The total capacitance of the preamplifier network was thus found to be 156 pF, while the total resistance was 400 GΩ.

For the case of the bimorphs, a resistivity of 1.5×10^{13} Ω m yielded resistance values of 2.25 GΩ for bimorph $B1$ and 7 GΩ for bimorphs B2 and B3. The capacitances of the three bimorphs were also measured, using a standard capacitance meter, and found to have values of 6.29, 2.47, and 2.3 nF for bimorphs $B1$, $B2$, and $B3$, respectively. These relatively high values are to be expected because the bimorph essentially consists of a stack of single-film elements. The resistance value for a thin single-film element is on the order of 10^2 MΩ, and its capacitance is on the order of 10^3 pF, depending on the electrical and geometrical properties of the particular film. From these values and the amplifier values measured above, we see that the circuit is dominated by the bimorph electrical parameters. We can then use Eqs. (10)–(12) to obtain values for R, C, and the electrical time constant τ_E of the bimorph circuit. The results of these calculations may be summarized as follows: for bimorph $B1$, $R = 2.24$ GΩ, $C = 6.45$ nF, and $\tau_E = 14.45$ s; for bimorph $B2$, $R = 6.88$ GΩ, $C = 2.63$ nF and $\tau_E = 18.09$ s; for bimorph $B3$, $R = 6.88$ GΩ, $C = 2.46$ nF and $\tau_E = 16.92$ s. From these considerations we see that the bimorph configuration yields a relatively slow response; the gain in sensitivity is achieved at the expense of the speed of the device. The electrical time constants of some pyroelectric films may be still higher,[17] however, on the order of 10^3 s. Like these detectors, the bimorph is suitable for quasi-static measurements at relatively low modulation frequencies.

III. EXPERIMENTAL RESULTS AND DISCUSSION

The general experimental arrangement for testing the pyroelectric bimorph detectors is shown in Fig. 3. A cw argon-ion laser (Coherent Innova 90) at 488.0 nm was used as the excitation source. Its output was modulated by an acousto-optic modulator driven by the internal waveform generator of a dynamic signal analyzer (Hewlett-Packard 3562A); the same signal is used as the reference to the lock-in amplifier (EG&G PARC 5210). The amplitude of the input waveforms to the acousto-optic modulator was 0.3 V; for this input voltage the modulator transmission ratio was about 0.02. The signal from the bimorph is processed by a wideband preamplifier (Ithaco 1201) with a variable gain, before being measured by the lock-in amplifier. The actual output power of the laser is measured by a fast photodiode located internal to the laser head, and is displayed on the front panel of the laser control unit. A feedback mechanism from this photodiode provides for stabilization of the output intensity.

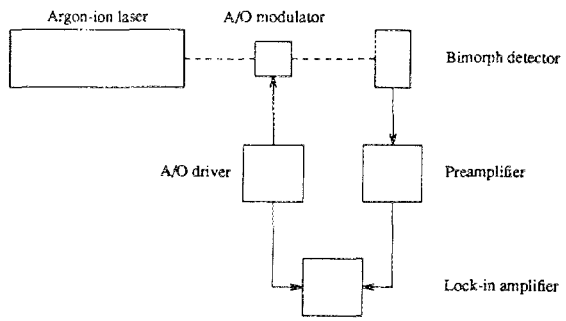

FIG. 3. Experimental arrangement for testing pyroelectric bimorph detector.

Figures 4(a)–4(c) show the measured bimorph output voltage against input laser power as 488.0 nm for modulation frequencies 23, 127, and 997 Hz, for bimorphs B1, B2, and B3. To a good approximation, the response of the bimorph detector is linear as expected from Eq. (3), and calibration of the device can be accomplished quite easily. Linear least-squares regression of the bimorph response with input laser power results in correlation coefficients ranging 0.987 to 0.999 The calibration factors may be obtained from the slope of the bimorph signal against laser power curve frequency. At 23 Hz, for example, this ranged from 0.12 V/W for bimorph $B1$ to 0.33 V/W for bimorph $B3$. The calibration factor for the $B1$ bimorph power monitor is 8566 ± 170 mW/V, at this modulation frequency. The percentage error in the calibration remained within $\pm 2\%$ for all experimental runs and modulation frequencies, a deviation which could be attributed to noise and detector repositioning error. Similar results were obtained for the other detector elements.

Figure 5 shows the responsivity ρ of the pyroelectric bimorph detectors as a function of modulation frequency. These plots were taken at a fixed laser power of 500 mW at 488 nm, using a 0–1-kHz frequency sweep input to the modulator and a dynamic signal analyzer (Hewlett-Packard 3562A) to recover the response. The roll-off of the responsivity at high frequencies is a characteristic of thermal detectors and, as well as being a calibration curve for modulation frequency, serves as an indication that the bimorph is indeed being operated in the pyroelectric mode. In contrast, the bimorphs exhibit a flat nonthermal response, with no high frequency roll-off, to a frequency-swept (0–1 kHz) acoustic waveform launched by a piezoceramic transducer (Archer 273-073)—a further indication that in the experiments reported here we were indeed operating in the pyroelectric rather than the conventional piezoelectric mode.

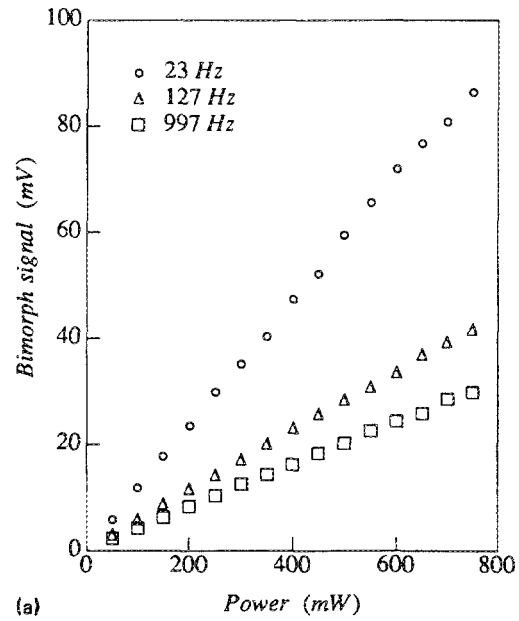

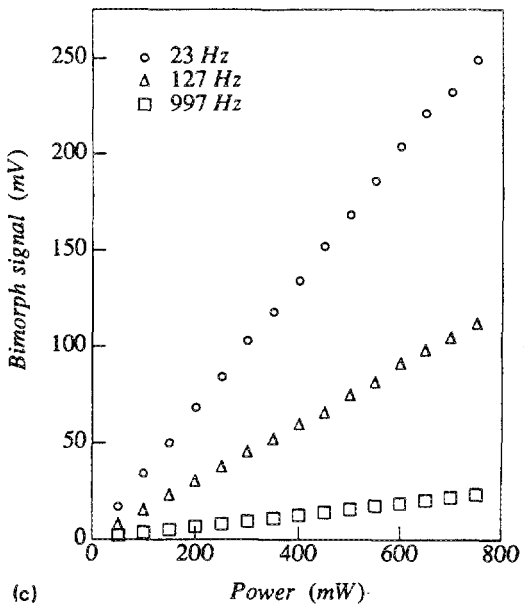

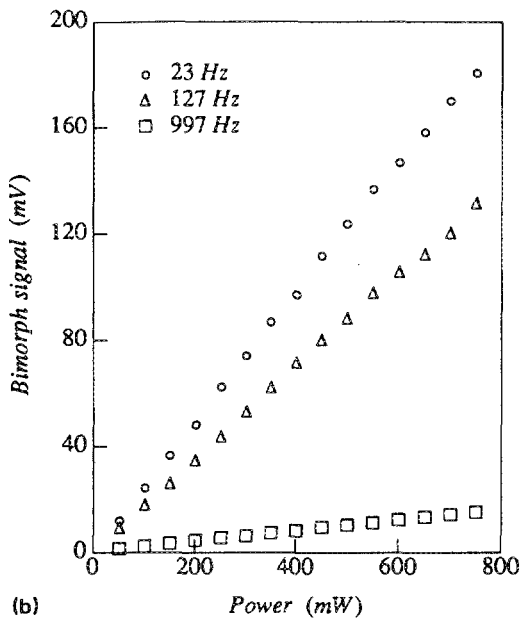

FIG. 4. (a) Voltage-power response of pyroelectric bimorph B 1. The data at 997 Hz has been multiplied by a factor of 50. (b) Voltage-power response of pyroelectric bimorph B 2. The data at 127 Hz has been multiplied by a factor of 5; at 997 Hz by a factor of 50. (c) Voltage-power response of pyroelectric bimorph B 3. The data at 127 Hz has been multiplied by a factor of 2.5; at 997 Hz by a factor of 50.

Although the responsivity effectively defines the sensitivity of a device it gives no indication of the minimum radiant flux that can be detected. This minimum detectable flux is defined as the rms incident radiant power required to produce an output signal V_s equal to the detector noise level V_n in other words, a signal-to-noise ratio of unity, and is known as the noise equivalent power NEP, given by

$$\mathrm{NEP} = \frac{P}{V_s/V_n} = \frac{V_n}{\rho}. \tag{16}$$

Since the higher the performance of the detector the lower the NEP, it is convenient to define the quantity D^*, the specific detectivity. This quantity is also convenient for comparing detectors of varying detector area, and is defined by

$$D^* = (A\Delta f)^{1/2}/\mathrm{NEP}, \tag{17}$$

where A is the area of the detector and Δf the bandwidth of the measurement. Values for the specific detectivity of the three devices are plotted in Fig. 6. The scatter in D^* was determined mainly by the scatter in the measured V_n. As expected, however, the three bimorphs display similar responses.

The maximum value for the specific detectivity for pyroelectric materials is given by[18] $D^*_{\mathrm{ideal}} = 1.8\times10^{10}$ cm $\mathrm{Hz}^{1/2}/\mathrm{W}$. Specific detectivity values as high as 3×10^8 cm $\mathrm{Hz}^{1/2}/\mathrm{W}$ at 1 Hz have been reported for single-film pyroelectric polymers,[15] although the values for specific films vary over a large range depending on the film manufacturing process. In our case, the pyroelectric bimorphs exhibited specific detectivities at 1 Hz of up to $D^* = 6.6\times10^8$ cm $\mathrm{Hz}^{1/2}/\mathrm{W}$ for bimorph B 3. This is approximately twice the value reported above for a single-film element.[15] It is notable that this gain in detectivity over single-film devices continues up to about 100 Hz; below the frequency the at-

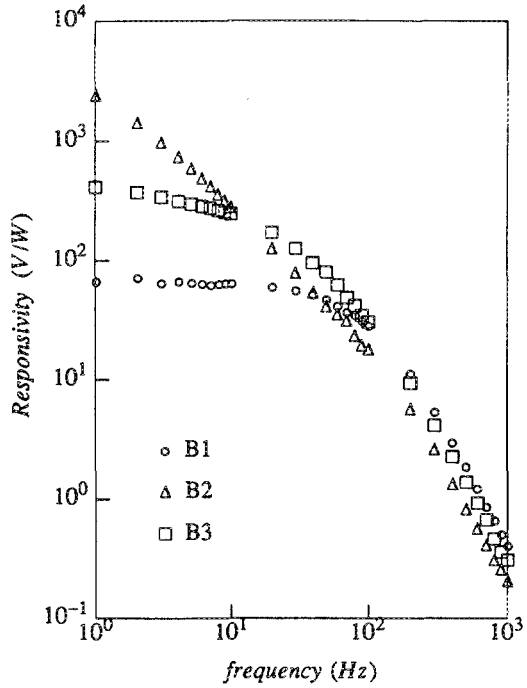

FIG. 5. Frequency response of pyroelectric bimorphs.

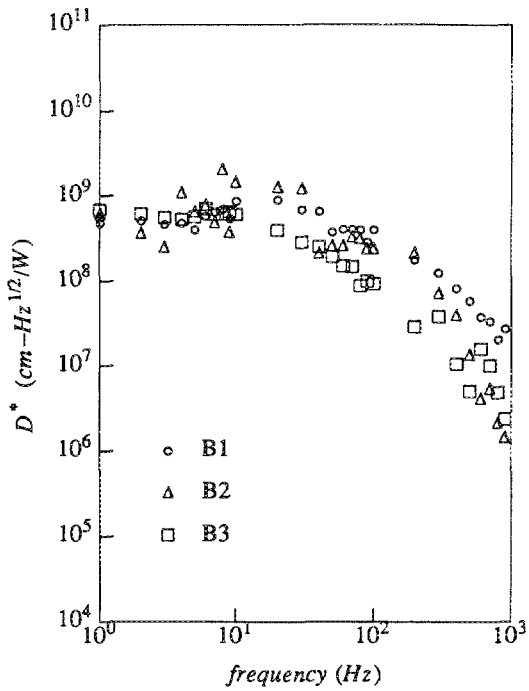

FIG. 6. Specific detectivity of pyroelectric bimorphs.

tenuation of the thermal field with detector depth is negligible and the effective current source is consequently amplified, as expected from Eq. (8). At higher modulation frequencies the thermal attenuation becomes larger, and the specific detectivity consequently decreases. The values in Fig. 6 do not necessarily determine the ultimate performance of PVDF bimorphs; the devices tested were found to have slightly inhomogeneous properties across their surface, possibly due to lamination or poling defects. This points out the possibility of increasing the performance of such devices even more through refinements of the fabrication process.

One possible problem with the use of polymer films as detector elements is their relatively low optical damage threshold. This difficulty may be overcome by attaching the bimorph to the rear surface of a thin metallic front plate, such as brass or aluminum. A similar strategy has been used previously in a piezoceramic detector.[19] Effectively the bimorph becomes a calorimetric detector, measuring the back-surface response of the heat diffusion through the laser-excited front plate. The signal output of the bimorph may then be analyzed in a manner similar to that used for single-element PVDF calorimetric detectors.[20,21]

It should be noted that the same theoretical analysis and general experimental configuration may be followed for multilayered pyroelectric films. Pyroelectric bimorphs and multimorphs are potentially useful in all areas where single-film detector elements are employed now. They can be used over a large spectral bandwidth, with the only requirement that the energy be absorbed at the detector front surface. Like their constituent films they can be used over a wide range of temperatures, have low-power requirements and preserve the advantage of low cost while having the potential of yielding devices of higher detectivity than their single-film counterparts.

ACKNOWLEDGMENTS

The authors wish to acknowledge the financial support of the Ontario Laser and Lightwave Research Center (OLLRC) for this work. Partial support from the Natural Sciences and Engineering Research Council (NSERC) of Canada is also gratefully acknowledged.

[1]T. T. Wang, J. M. Herbert, A. M. Glass, Eds., *The Application of Ferroelectric Polymers* (Chapman and Hall, New York, 1988).
[2]P. N. J. Dennis, *Photodetectors* (Plenum, New York, 1986).
[3]R. L. Byer and C. B. Boundy, Ferroelectrics **3**, 333 (1972).
[4]A. Ballato and E. A. Gerber, Eds. *Precision Frequency Control* (Academic, New York, 1985).
[5]H. Kawai, Jpn. J. Appl. Phys. **8**, 975 (1969).
[6]M. Toda and S. Osaka, Trans. IECE Jpn. E-61, 507 (1978).
[7]M. Toda, Trans. IECE of Jpn. E-61, 513 (1978).
[8]M. Toda, Ferroelectrics **32**, 127 (1981).
[9]M. Toda, IEEE Trans. Electron Devices **ED-26**, 815 (1979).
[10]D. H. Dameron and J. G. Linvill, Sensors and Actuators **2**, 73 (1981/82).
[11]J. G. Bergmann, J. H. McFee, and G. R. Crane, Appl. Phys. Lett. **18**, 203 (1971).
[12]A. C. Tam and H. Coufal, Appl. Phys. Lett. **48**, 33 (1983).
[13]K. Tanaka, Y. Ichimura, and K. Sindoh, J. Appl. Phys. **63**, 1815 (1988).
[14]M. Mieszkowski, K. F. Leung, and A. Mandelis, Rev. Sci. Instrum. **60**, 306 (1989).
[15]E. H. Putley, Infrared Phys. **20**, 149 (1980).
[16]H. J. Coufal, R. K. Grygier, D. E. Horne, and J. E. Fromm, J. Vac. Sci. Technol. **A5**, 2875 (1987).
[17]Technical Manual, Kynar Piezo Film, Pennwalt Corporation, Valley Forge, PA.
[18]R. J. Phelan, R. J. Matler, and A. R. Cook, Appl. Phys. Lett. **19**, 337 (1971).
[19]S. B. Peralta, H. H. Al-Khafaji, and A. W. Williams, J. Phys. E. **21**, 195 (1988).
[20]A. Mandelis, Chem. Phys. Lett. **108**, 388 (1984).
[21]H. Coufal, IEEE Trans. Ultrason. Ferroelectr. Frequency Control UFFC-33, 507 (1986).